ILASS 2008
Sep. 8-10, 2008, Como Lake, Italy

Paper ID ILASS08-2-12

ON PERFORMANCE OF ADVECTION SCHEMES IN THE PREDICTION OF DIESEL SPRAY AND FUEL VAPOUR DISTRIBUTIONS

Fabian Peng Kärrholm, Feng Tao

+46-31-7725032, fabian.peng-karrholm@chalmers.se
Chalmers University of Technology

ABSTRACT
We have investigated the performance of advection schemes (focusing mainly on Total Variation Diminishing, TVD, schemes) applied in modelling diesel sprays, and assessed their influence on liquid spray penetration and fuel vapour distribution. Here, we compare sprays simulated using several types of TVD schemes (Superbee, MUSCL, limited Linear, and UMIST) – and standard upwind and linear schemes as references – in conjunction with three different turbulence models (standard, RNG and Launder-Sharma k-ε models), to non-reacting diesel sprays observed in the Sandia high-pressure, high-temperature constant-volume vessel. The OpenFOAM CFD code was used for all of the simulations described. In addition to comparing the simulations to experimental data, we provide overall assessments of the performance and utility of the TVD schemes in multi-dimensional diesel modelling.

INTRODUCTION

Modelling of reactive flows in compression- and spark-ignition engines, has advanced considerably in the last 25 years and has become an important component of engine research and development efforts. The KIVA family of CFD codes has gained popularity amongst members of the global engine research community in industrial, academic and government facilities, due to its generally good performance in numerical modelling. KIVA-3 applies Arbitrary-Lagrangian-Eulerian (ALE) methodology in a structured mesh of hexahedrons [1]. The Navier-Stokes equations are solved on a staggered grid, which restricts the solver to Cartesian meshes. The equations of conservation and turbulence are treated using an operator-splitting technique, in which the diffusion and source terms in the equations are split and solved by a conjugate residual method in a coupled, implicit manner. The remaining terms (convective transport) are computed by a quasi-second-order-upwind (QSOU) scheme, or partial donor cell (PDC) scheme.

When fluid problems become more complex, in terms of geometry and structure, Cartesian meshes are too limited. Therefore, collocated grid solvers are more commonly applied by modern solvers such as STAR-Adapco [2], Fluent [3], OpenFOAM [4] etc. A finite-volume, collocated grid structure allows for polyhedral cells of arbitrary shape, and thus the ability to mesh arbitrarily shaped structures.

Modern CFD codes have demonstrated utility for modelling flows of fluids, both compressible and incompressible, in diverse contexts. However, simulating transient, multiphase diesel sprays and combustion systems still poses several challenges. For example, in a recent study [5], we compared the performance of OpenFOAM and KIVA-3 for simulating multiphase diesel sprays and flames in a high-pressure, high-temperature constant-volume vessel, and found that OpenFOAM appeared to over-predict the penetration length of the diesel flame, while KIVA-3 yielded predictions that were closer to measured data.

Objectives

The objectives of the work reported here were to improve the modelling of diesel flames in engine-like conditions, and improve the performance of OpenFOAM. We have previously assessed the influence of grid, time step, and the turbulence model on the liquid and vapour penetration [6,7] and flame development [5]. Here, we address the influence of another numerical source, the advection scheme, on the numerical solution.

We compare results obtained from CFD simulations using different turbulence models and advection schemes to experimental data of a single-component n-heptane spray. In order to focus on the effects of schemes and turbulence models in isolation, the sprays considered are all non-combusting sprays, since combustion affects the solutions by generating pressure waves, large temperature rise, and changes in density due to the temperature rise. Thus, simulating non-combusting sprays of a single-component fuel allows simplification without compromising the ability to verify the results experimentally. It is also important to ensure the code reproduces fuel vapour distributions sufficiently accurately, if it is going to be used to calculate combustion processes, otherwise there will be substantial errors.

SPRAY PHYSICS

Combustion and emissions formation in diesel engines are the results of chemical reactions of diesel fuels in high-pressure, high-temperature environments. In conventional direct-injection (DI) diesel operation, a single spray is injected into an engine cylinder where it undergoes several physical processes – atomization, droplet breakup, coalescence, turbulent dispersion, droplet evaporation, vapour diffusion and convection, etc. Consequently, the fuel vapour from the spray mixes with the air charge and, after a very short delay, ignition may occur at the sites with a favourable mixture and thermodynamic conditions. These processes propagate,

leading to post-ignition flame development, determining flame lift-off, quenching and re-ignition, and ultimately controlling emissions formation and oxidation in diesel engines.

Despite the complexity of diesel processes, in conventional diesel operation heat is released in a stable, typical pattern, with two distinct phases: a premixed phase and a mixing-controlled phase. The premixed phase is a result of fast, spontaneous reactions of the vaporized fuel and air mixture. It is characterized by a rapid rise in the apparent heat release rate, lasting only a few crank angle degrees after ignition. In the mixing-controlled phase, mixing of the fuel and the ambient charge becomes a dominant factor that limits the rate of heat-release-controlling reactions, and the apparent heat release rate curve changes gradually over a relatively long crank angle period.

Quantitative knowledge of liquid spray penetration and fuel vapour distribution is essential for understanding (and thus developing the ability to control) ignition, heat release, and emissions formation processes in diesel engines. In order to obtain such understanding, many measuring techniques (e.g., Mie-scattering and shadowgraph imaging) have been applied to measure liquid penetration and vapour distribution, for example, in a quiescent, high-pressure, high-temperature**,** constant-volume vessel by Siebers *et al*. [8] and in an optically-accessible, heavy-duty diesel engine by Dec *et al*. [9]. These studies have revealed that: (a) the liquid length decreases linearly with orifice diameter and approaches zero as the orifice diameter approaches zero; (b) injection pressures up to 140 MPa have no significant effect on the liquid length; (c) the liquid length decreases with increasing ambient gas density (up to 59 kg/m^3) or temperature (up to 1300 K); and (d) in a diesel flame the liquid length is only about 25 mm, while the fuel vapour penetrates a little further than the spray tip, forming a mixture with an equivalence ratio of 3-4.

NUMERICS

Accurate prediction of the fuel vapour distribution of diesel sprays is crucial in multidimensional diesel modelling. The ways in which the fuel vaporization, convection and diffusion is modelled will have major effects on the ignition, flame, and resulting emissions formation simulations. If the scheme does not convect the fuel away from the injector, or the fuel is allowed to diffuse upstream to the injector, the distance between the injector and flame (flame lift-off length) will be unrealistic. It is therefore important for the scheme to both properly represent the air entrainment, and be able to handle the large gradients between quiescent air and entrained air. Air entrainment and fuel/air mixing are essentially problems of high concentration gradients involving both fuel vapour and ambient air.

When simulating complex flows, it is often desirable to use a high order scheme to achieve good predictions with low errors. However, as the order of the scheme is increased it becomes unbounded, which can cause non-physical oscillations and overshoots/undershoots, especially around high gradient regions. To maintain boundedness, one of the few options is to use an upwind scheme, but this is associated with rather large diffusive truncation errors [10]. Therefore, it is beneficial to use a high order scheme in the parts of the domain where it will not lead to an unbounded solution, and an upwind/downwind scheme in the high gradient regions to maintain boundedness.

TVD Schemes – background

Schemes that remain bounded while using higher order interpolation than upwind/downwind schemes are Total Variation Diminishing (TVD) schemes, which were developed from Lax-Wendroff schemes, via Lax-Friedrich and Flux-Corrected Transport (FCT) schemes, to handle problems relating to high gradients in flows [11]. The TVD schemes are based on the criteria that the formation of new local extreme points should not be allowed, existing maxima should not be allowed to increase, and existing minima should not be allowed to decrease. In mathematical terms, the TVD condition for a variable U can be stated as follows (*n* is the time index):

$$TV(U^{n+1}) \le TV(U^{n}) \tag{1}$$

where TV is the total variation of the function. For a 1D case this is reduced to (*i* is the spatial index):

$$\sum_j \left| U_{j+1}^{n+1} - U_j^{n+1} \right| \le \sum_j \left| U_{j+1}^{n} - U_j^{n} \right| \tag{2}$$

They are often used to predict shocks in compressible supersonic flow calculation. We consider how TVD schemes work in detail in the modelling section.

The two features of TVD schemes mentioned above are beneficial for most simulations of physical quantities, since they are consistent with the laws of physics. For instance, a quiescent cloud of fuel will slowly diffuse rather than become more concentrated, its maximum concentrations will not increase and new local maxima will not form. Since TVD schemes always follow these conditions they will not produce solutions that are non-physical in this sense, and their solutions will be free of spurious oscillations.

Numerical simulation of Diesel Sprays

Numerical simulations of diesel sprays are affected by other factors in addition to the numerical scheme, e.g. the sub-models used for the spray processes, and the grid used for the discretization. Sub-models are used in Eulerian-Lagrangian simulations to describe each of the processes mentioned in the previous section that the liquid undergoes. The choices of sub-models, grids and discretization procedures affect not only the vapour distribution, but also ignition delay time and site, flame development, lift-off length, emissions formation, and oxidation in diesel engine simulations.

A major difficulty when simulating sprays is to get all these factors to work cohesively, and produce good results that match experimental data. In order to do this, the results are often tuned, since almost every sub-model contains several numerical constants that can be altered to fit empirical data. In the work reported here one set of values was chosen for all of the simulations, but it would probably be possible to alter the constants and obtain good results with other turbulence models, other schemes and other initial values for variables such as k, epsilon and droplet sizes.

Discretization of the Advection Term

The ability to select a scheme at runtime has been exploited to investigate the effect of the numerical scheme chosen for the advection term, more specifically, the second term on the left hand side in the momentum equation:

$$\frac{\partial \rho U}{\partial t} + U^T \cdot \nabla(\rho U) = -\nabla p + \nabla \cdot (\mu_{Eff} \nabla U) + F \quad (3)$$

Superscript T indicates transpose of vector. These terms are discretized using the finite volume method, and after applying the Gauss theorem to the second (advection) term it becomes:

$$\sum_{\text{faces of cell P}} (\rho_f \vec{U}_f^T \cdot n_f) A_f (U)_f \quad (4)$$

where A_f is the area, n_f the normal vector, ρ_f the density, and $\vec{U}_f^T$ the velocity at face *f*. The second U in the equation is the unknown velocity in the x, y, and z direction, also evaluated at face *f*. It is calculated when solving equation 3 in x, y, and z, respectively.

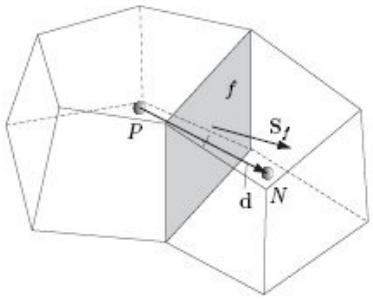

Figure 1. Illustration of two adjacent cells, P and N. Sf is the cell face area vector of face f (S_f=$A_f n_f$), and *d* is the cell-centre distance. Reprinted from [12].

From equation 4 it can be seen that the face values of all variables are required. They are obtained through interpolation of the cell-centred values. The way in which this interpolation is done will have a large impact on the solution, as shown below. We will focus on interpolation of the last variable, $(U)_f$. For a more detailed description of how the interpolation is done etc, see [13]. The general equation for the face value of face *f* is (for notation see Figure 1):

$$U_f = \lambda (U_P - U_N) + U_N \quad (5)$$

λ is a weighting factor which will determine the kind of interpolation that will be used. Note that this equation is valid for all schemes that only consider the nearest cells, it is not limited to TVD-type schemes. For equidistant meshes, λ is:

$$\lambda = \frac{1}{2} r + (1 - r)\chi \quad (6)$$

where χ is 1 if we have flux out of the cell, and 0 otherwise. *r* is determined by the scheme; some examples are given below. More than 40 numerical schemes are available in OpenFOAM for interpolation of a variable, nine of which are TVD-type schemes. TVD schemes require calculation of the TVD variable which is limited in different ways depending on the chosen scheme. The TVD variable for a variable U is defined as (positive face flux indicates flow from cell P to N**,** as shown in Figure 1):

$$R_f = \begin{cases} 2\dfrac{d \cdot \nabla |U_P|}{|U_N| - |U_P|} - 1 & faceflux > 0 \\ 2\dfrac{d \cdot \nabla |U_N|}{|U_N| - |U_P|} - 1 & faceflux \le 0 \end{cases} \quad (7)$$

where *d* is the distance between the centres of the two cells involved. Since U is a vector, the magnitude is used, as R needs to be a scalar. The term in the numerator is evaluated by linear interpolation of the cell values to the faces, and then calculating the gradient at the cell centre. The variable *R* provides information on the extent of the variation of |U| over the neighbouring cells compared to over the current and adjacent cells. It is then limited by different functions depending on the scheme chosen, and it should be noted that this is the only difference between the schemes. In this contribution we have focused on four TVD-type schemes, which are listed below.

TVD Limiters considered here

The r calculated according to the equations below is used in equation 6.

Monotonized Central (MC)

This scheme [14] is implemented in OpenFOAM under the name MUSCL, which is unfortunate since MUSCL generally refers to a whole branch of schemes. It is an abbreviation for Monotone Upwind Centered Schemes for Conservation Laws.

$$r = \max(\min(2R, \frac{1}{2}R + \frac{1}{2}, , 2), 0) \quad (8)$$

Limited Linear

This scheme is an OpenFOAM "invention", so there is no reference for it. k is set by the user at a value between 0 and 1 (usually 1). r is then limited to:

$$r = \max(\min(\frac{2}{k}R, 1), 0) \quad (9)$$

SuperBee

SuperBee [15] uses the following flux limiter

$$r = \max(\min(2R, 1), \min(R, 2), 0) \quad (10)$$

UMIST

UMIST [16] has a large flux limiter:

$$r = \max(0, \min(2R, 2, (0.75R + 0.25), (0.25R + 0.75))) \quad (11)$$

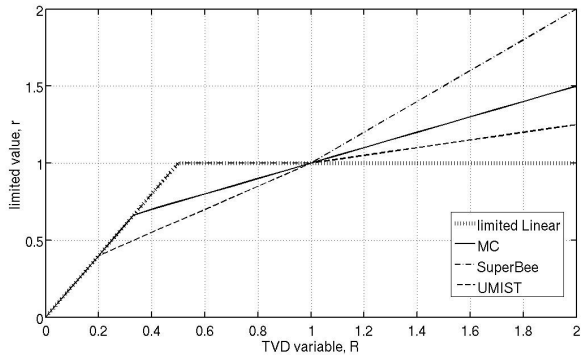

Figure 2. Comparison of the four considered limiter functions, *r*, with respect to the TVD variable, *R*. The SuperBee scheme overlaps the limited Linear scheme for *r* values between 0 and 1. 0, 1, and 2 values of *r* correspond to pure upwind, central differencing and downwind schemes, respectively.

As can be seen from all of the limiters, the flux variable is never allowed to exceed 2 (or 1, in the case of limited Linear), nor go below zero. If r is 0 the upwind scheme will be used, and if it is 2 the downwind scheme. For smooth functions, the property in equation 7 is unity, which causes TVD schemes to use a higher order interpolation (central differencing). This is because when r is not unity, it indicates that the function has a sharp gradient, or is close to a zero-gradient point (i.e. the numerator in equation 7 is close to zero). Thus, UMIST, SuperBee and MC can all use some downwinding, whereas limited Linear uses only upwind and central differencing. To visualize how the different schemes limit the flux variable, the four limiter functions are plotted in Figure 2, which shows (together with equation 6) how the schemes switch between upwind, central and downwind.

Example of effects of different TVD limiters

An example of a theoretical case where downwind would be used is shown in Figure 3, which could illustrate the velocity in the spray direction, with an early maximum speed that subsequently slowly declines back down to zero. As the fluid is decelerated due to the wall at position 6, SuperBee will acknowledge the wall earlier than limited Linear does, by using downwind at positions 4 and 5. If we look at the acceleration part, upwind is used when there is a sudden acceleration, as at position 1, and linear is used when the acceleration is steady, as at position 2.

There are many other limiter functions, mainly because no single method is suitable for addressing all problems. The optimal method is problem-specific, and the best one must be found for each problem.

In addition to the schemes mentioned above, upwind and the linear scheme were included for reference purposes.

Fuel	n-heptane
Injection Pressure	150 MPa
Fuel Temperature	373 K
Nozzle Diameter	0.1mm
Ambient Temperature	1000 K
Ambient Density	14.8 kg/m3
Ambient Gas Composition	O_2:N_2:CO_2:H_2O = 0:90:6.5:3.5

Table 1. Summary of Experimental Conditions

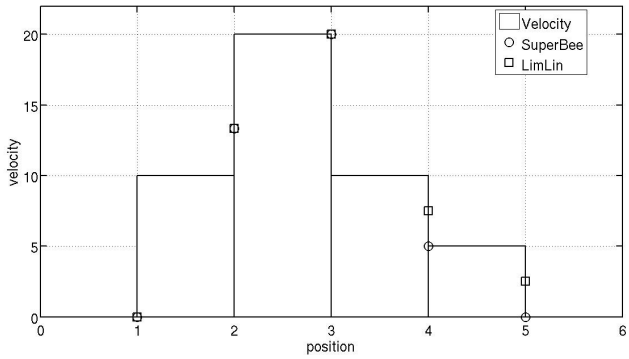

Figure 3. Simple example of flow in six cells, cellular values displayed by the bars, and interpolated face values displayed by circles or squares depending on the scheme chosen for interpolation. Both schemes use upwind for faces at points 1 and 3, with central differencing at point 2, but SuperBee uses downwind in 4 and 5, while limited Linear uses central differencing.

NUMERICAL SETUP

The simulations have been conducted using OpenFOAM CFD code, an objected-oriented open source code written in C++. The code supports polyhedral meshes, face-to-face tracking of Lagrangian parcels, with a fully-coupled chemistry solver, runtime selection of all sub-models and parallelization of computations.

Euler-Lagrangian spray simulations use two different kinds of descriptions for the vapour/gas and the liquid. Various sub-models are then needed to simulate the interactions between these two phases, in this work the same sub-models as listed in [5] were used.

Since the grid can also have a large influence on the simulations, three different grids were tested to investigate grid effects. The grid spacing close to the injector (where liquid parcels are introduced) was found to have a large effect on the spray development. For the standard mesh, around 130 000 cells were used. The cell size around the injector was then 1.35 mm by 0.85 mm. It is shorter in the radial direction as it is believed to have a large influence on the spray development.

SETUP FOR THE TEST CASE

The empirical data chosen to assess the validity of the simulations originate from experiments performed at Sandia National laboratories [8], in which an n-heptane spray was injected into an optically-accessible, high-pressure, high-temperature, cubical, constant-volume vessel with 108 mm sides designed to represent quiescent diesel engine conditions. As mentioned above, we focus here on non-reacting sprays, and compare observed and simulated vapour distributions and liquid spray penetrations. Hence, the data used are liquid penetration and fuel distribution measurements obtained for a case with 0 % oxygen. The experimental conditions are summarized in Table 1, and also available online in the Engine Combustion Database (ECN).

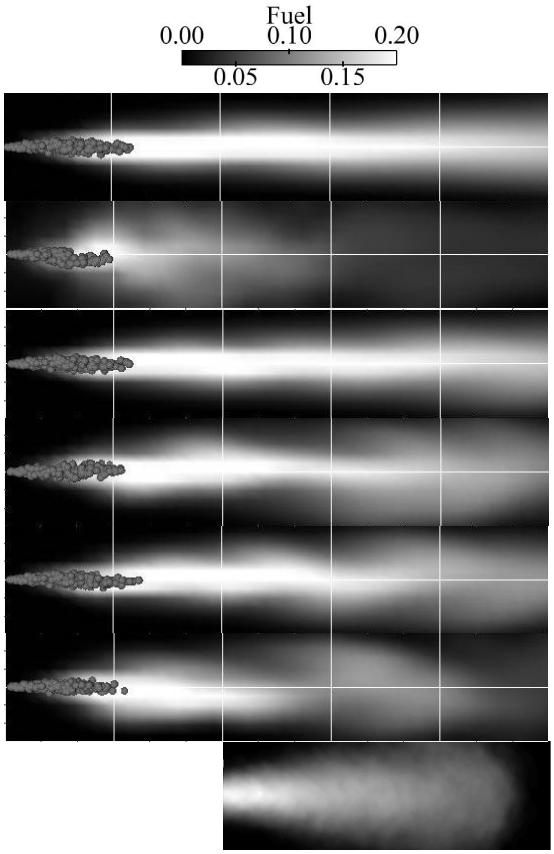

Figure 4. Vapour distributions of n-heptane in the central plane, 0.9 ms after SOI, obtained using the RNG k-ε turbulence model and the following five advection schemes, from top: upwind, linear, Limited Linear, MC, UMIST, SuperBee, and experimental values. Initial μ_T= $3.75 \cdot 10^{-4}$ m^2/s.

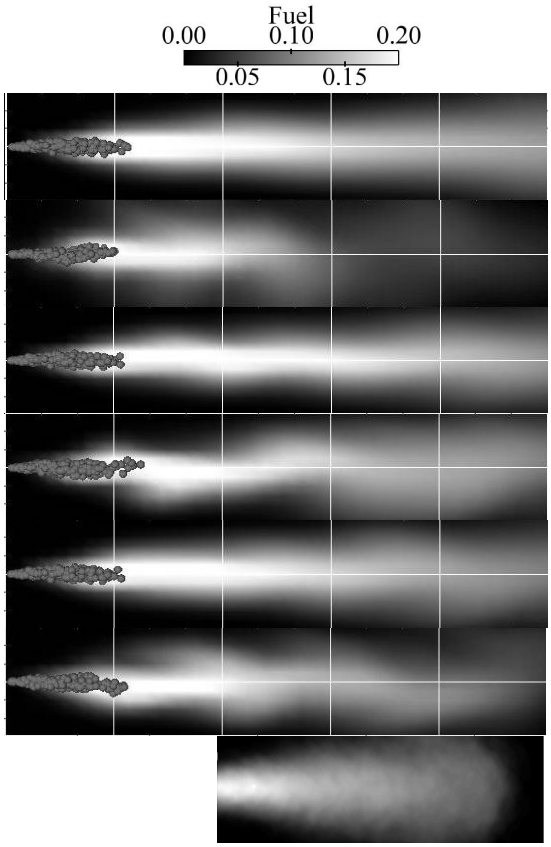

Figure 5. Vapour distributions of n-heptane in the central plane, 0.9 ms after SOI, obtained using the Launder Sharma k-ε turbulence model and (from top) the upwind, linear, limited linear, MC, UMIST and SuperBee schemes for the advection term. A corresponding distribution obtained in experiments is shown in the bottom image.

RESULTS AND DISCUSSION

The simulations were run using three turbulence models; standard k-ε, the Renormalized Group k-ε model and the Launder Sharma modification of the k-ε model. Due to space limitations the standard k-ε has been left out. All images are 10 mm wide and show white lines at 10 mm intervals in the spray direction, unless other stated.

As can be seen in Figure 4, there are large differences in the results obtained with the different schemes in terms of both vapour penetration length and structure of the vapour distribution. This is an important feature, indicating that the turbulence model can represent the unsteadiness present in the fuel spray. Even though the RNG k-ε model is an eddy viscosity model which is designed to model all turbulence in each cell at a single scale, it is able to account for the different scales of the turbulence by altering the production term. The experimental distribution shown is averaged over 30 sprays.

If the Launder Sharma k-ε model is used, there are also differences, but the model is slightly more diffusive than the RNG turbulence model, especially for high initial k and low initial ε values.

There are clear between-scheme differences at low viscosities, as shown in Figure 5. Notably, the linear scheme may seem to provide a better solution than the others in terms of fuel vapour distribution lengths, however examination of the simulated velocity field (Figure 6) shows that the solution is full of "wiggles" and non-physical instabilities. The situation is similar when RNG is used with the linear scheme, and such instabilities arise whenever large gradients are present.

The simulation obtained using the Superbee interpolation scheme is quite different (Figure 5). It shows instabilities, but not to the same degree as the pure linear simulation, and the velocity results show it provides a smooth, stable solution (not shown).

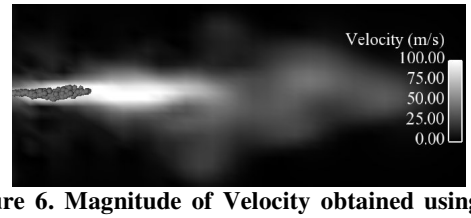

Figure 6. Magnitude of Velocity obtained using linear interpolation of the advection term. Non-physical wiggles can be seen around the injector.

If the simulations are tuned to match experimentally measured vapour penetration using the Launder Sharma k-ε model, the spray becomes steadier, and the differences between the schemes are almost eliminated. This is believed to be associated with the high viscosity introduced by the turbulence model. If the solution is smoothed by the turbulence model, the limiter variable will be unity for all cells, and the choice of limiter will not have any influence on the solution, see Figure 7. A time-sequence of the vapour

distribution obtained using the Launder Sharma k-ε model for modelling turbulence and SuperBee for the advection term, and tuned to match experimental data, is shown (together with an experimentally obtained image of a corresponding spray) in Figure 9.

As seen in Figure 7, and when comparing Figure 5 and Figure 9, there is a large difference obtained from varying initial turbulent viscosity. The problem is that, unlike temperature or pressure, the "real" initial turbulent viscosity is not known. It is also highly questionable whether or not this information is attainable, as the viscosity itself is a theoretical construction, and the k-ε type of models used are very simple models of an extremely complex phenomenon.

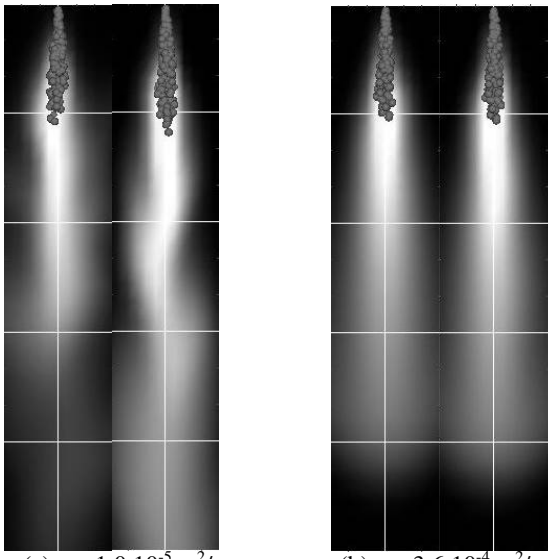

(a) $\mu_T=1.0\cdot10^{-5}$ m^2/s (b) $\mu_T=3.6\cdot10^{-4}$ m^2/s

Figure 7. Fuel Vapour distribution of four sprays. Sprays on the left in (a) and (b) uses linear interpolation, and the right uses MC interpolation. Launder-Sharma k-ε used for modelling turbulence. 1ms after SOI.

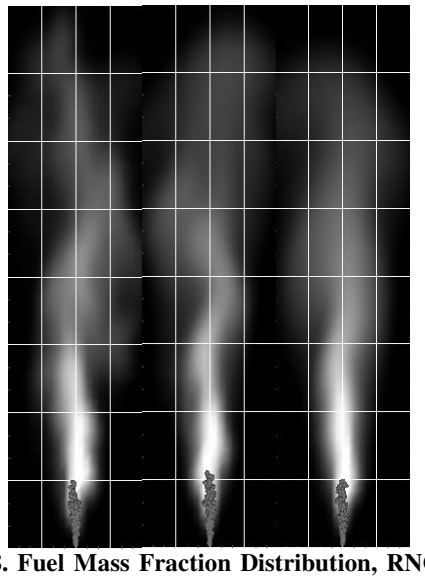

Figure 8. Fuel Mass Fraction Distribution, RNG (left), Launder-Sharma (middle), and standard k-ε turbulence models used. 2 ms after SOI. The images use the same scale as other images, but zoomed out as spray is further developed at 2 ms. Initial turbulence viscosity $\mu_T=1.0\cdot10^{-5}$ m^2/s.

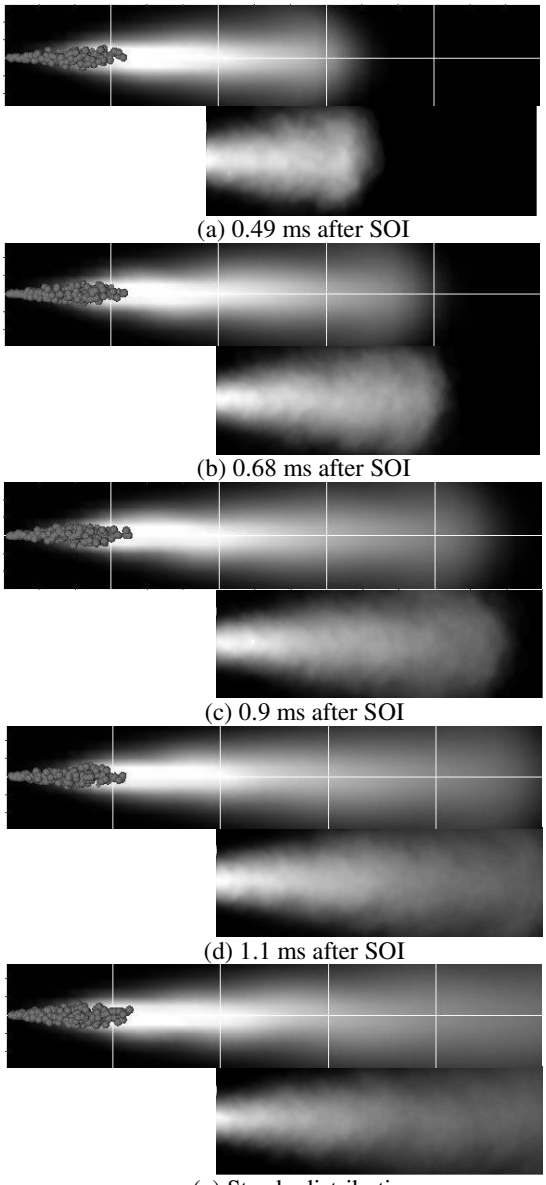

(a) 0.49 ms after SOI

(b) 0.68 ms after SOI

(c) 0.9 ms after SOI

(d) 1.1 ms after SOI

(e) Steady distribution

Figure 9. Vapour distribution of n-heptane in the central plane, 0.9 ms after SOI, obtained using the Launder Sharma k-ε turbulence model and the SuperBee scheme for the advection term. Tuned for experimental comparison; initial $\mu_T=1.15\cdot10^{-4}$ m^2/s. Corresponding distributions obtained in experiments are shown below each simulated distribution.

While this procedure provides a very good comparison to experimental results, it removes all unsteadiness and produces a smooth, averaged spray. This is satisfactory for bomb sprays, especially when there is no combustion. However, in a real engine, the spray will be influenced by several sources of disturbance, notably: turbulence in the cylinder is more intense due to the gas-exchange and the piston bowl movement; the injection profile is less flat and much shorter than the one used here; and last, but by no means least, the combustion will also disturb the spray. A satisfactory turbulence model and scheme should work well both for bombs and engine simulations.

To further compare the numerical and experimental results, radial values of the fuel mass fraction were plotted against numerical values obtained for corresponding points along the

laser sheet used to extract the time-averaged images shown above. The numerical simulations are not averaged in time, but along a line in the x&z-direction.

From Figure 8, it seems that the turbulence model has a low influence over the fuel vapour distribution. However, the radial plots shown in Figure 10, visualize it more clearly. The advection scheme has a larger initial effect on the fuel mass distribution than the turbulence model but later, when the spray has had more time to interact with the surrounding turbulent flow, the turbulence model starts to affect the results more strongly. After 1.1 ms, the distribution is affected by both the advection scheme and the turbulence model. Use of the Launder Sharma k-ε model with SuperBee manages to capture the distribution better than the others, all of which underpredict the width of the distribution. Similar trends can be seen in Figure 12, notably that limited linear over-predicts the liquid penetration.

Since the above mentioned combination seems to produce good results, it was used for the simulations illustrated in Figure 11. These two plots show the distribution at three distances from the injector 0.9 ms after start of injection (SOI). When SuperBee is used together with the Launder Sharma k-ε model, the distribution is fairly well predicted for all three distances from the injector. However, when RNG is used, it seems that although the simulation provides good predictions close to the injector (at 20 mm), the predictions become worse downstream, where the turbulence model has had a larger influence on the spray.

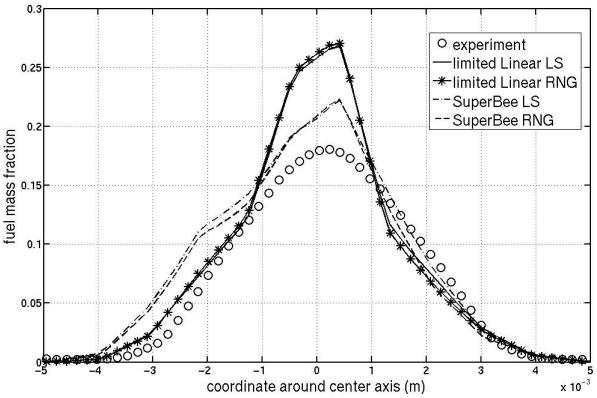

(a) 0.49 ms after SOI

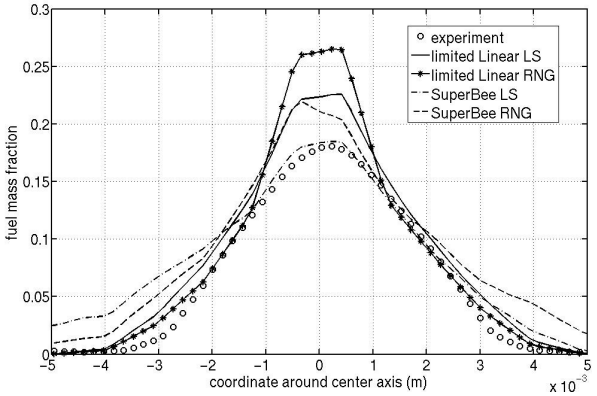

(b) 1.1 ms after SOI

Figure 10. Fuel Mass Fraction vs. distance from the centre axis, 20 mm from the injector

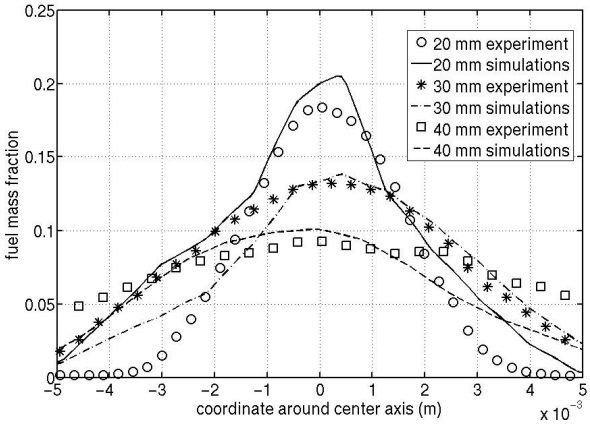

(a) Launder Sharma turbulence Model

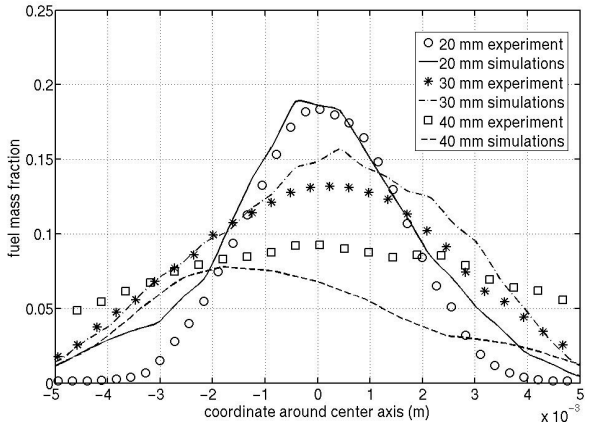

(b) RNG turbulence Model

Figure 11. Fuel Mass Fraction vs. distance from the centre axis, obtained using the SuperBee interpolation scheme for the advection term. Time, 0.9 ms after SOI

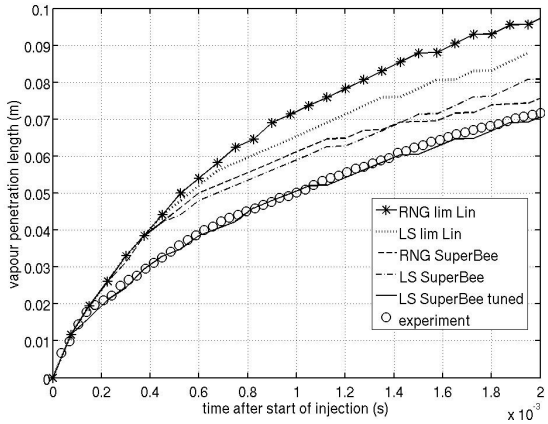

Figure 12. Liquid penetration lengths obtained using two different advection schemes, and two different turbulence models, compared to experimental data

Simulations have also been run on different grids to examine the effect of the cell size, see Figure 13. . As previously reported by several other researchers [18], decreasing the cell size causes the liquid and vapour penetration lengths to increase. In this case, the vapour distribution also becomes thinner, hence the distribution is widest when the coarsest grid is used. The results were found to be fairly grid independent when a high initial turbulent viscosity was used. The 130 000 cell grid was chosen for further analyses since sprays generated with this grid were not

as over-wide as those generated with the coarse grid, while their liquid penetration lengths were not as long as those generated with the fine grid.

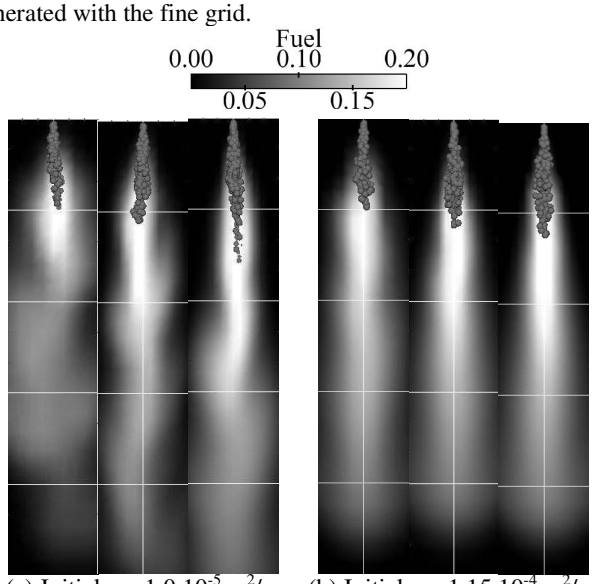

(a) Initial $\mu_T=1.0\cdot10^{-5}$ m^2/s (b) Initial $\mu_T=1.15\cdot10^{-4}$ m^2/s

Figure 13. Grid study using SuperBee interpolation on the advection term, and Launder Sharma k-ε for turbulence. Three grids used, and two initial turbulent viscosities was used, left grid has 80 000 cells, middle 130 000 cells and right 180 000 cells.

CONCLUSIONS

We have used a test case of a non-reacting diesel spray, which is injected into a high-pressure, high-temperature constant-volume vessel, to show that the choice of numerical scheme for the advection term can have profound effects in certain diesel spray simulations. If a diffusive turbulence model is chosen, or if very high initial turbulent viscosities are present, the choice of scheme becomes unimportant. However, if a transient spray is to be simulated, a turbulence model that can capture the transient effects is needed, and a scheme that does not dampen fluctuations as too much upwind will do. Situations in which transient spray simulations would be needed include attempts to model sprays associated with pilot-main injections and multiple injection strategies, in which it will be important to model the effects of previous sprays and the proximity of each spray correctly. Another important example is when misfires are studied, if every injection is the same, the spray model will never capture it.

Use of downwind in some of the schemes has a strong effect on the stability of the spray. One example of where downwind might be used (if the scheme allows), is in the core of the spray (the flow decelerates in the radial direction as it approaches the core), and by the tip of the spray, where use of linear or upwind schemes can lead to over-penetrating sprays. SuperBee was found to be suitable for spray simulations, since it does not over-predict the length of the vapour distribution, forming a fairly wide spray that is not too diffusive.

If diesel sprays are to be modelled predictably, and accurately, it is important not to rely on the turbulence model smoothing out the solution. Diesel Sprays are inherently unsteady, and it is the authors' belief that these instabilities need to be resolved to properly predict spray behaviour.

ACKNOWLEDGEMENTS

This work was supported by the Combustion Engine Research Center, at Chalmers. The authors are grateful to Lyle Pickett for providing experimental data, and to Drs. Niklas Nordin and Jonas Edman for valuable comments. The computations were performed using C^{3}SE computing resources, at Chalmers.

REFERENCES

1. Amsden, A.A., KIVA-3: A Block-Structured KIVA Program for Engines with Vertical or Canted Valves, Los Alamos National Laboratory, Report LA-13313-MS,1997.
2. http://www.cd-adapco.com/
3. http://www.fluent.com/
4. http://www.opencfd.co.uk/
5. Peng Kärrholm, F., Tao, F., and Nordin, N., Three-Dimensional Simulation of Diesel Spray Ignition and Flame Lift-Off Using OpenFOAM and KIVA-3V CFD Codes, *SAE Paper 2008-01-0961*, 2008.
6. Peng Kärrholm, F., Numerical Modelling of Diesel Spray Injection and Turbulence Interaction, Lic. Eng. Thesis, Chalmers Tekniska Högskola, Göteborg, 2006.
7. Peng Kärrholm, F., and Nordin, N., Numerical Investigation of Mesh/Turbulence/Spray Interaction for Diesel Applications, *SAE Paper 2005-01-2115*, 2005.
8. Siebers, D.L., Liquid-Phase Fuel Penetration in Diesel Sprays, *SAE Paper 980809*,1998.
9. Dec, J.E., A conceptual model of DI diesel combustion based on laser-sheet imaging, *SAE Paper 970873*, 1997.
10. Ferizger, J.H., and Peric, M., Computational Methods for Fluid Dynamics, Springer, 1999.
11. Laney, Culbert B., Computational gas dynamics, Cambridge University Press, 1998.
12. OpenFOAM Programmer's Guide, Version 1.4.1, OpenCFD, 2007.
13. Peng Kärrholm, F., Numerical Modelling of Diesel Spray Injection, Formation, Combustion and Turbulence Interaction, Ph.D. Thesis, Chalmers Tekniska Högskola, Göteborg, 2008.
14. van Leer, B., Towards the ultimate conservative difference scheme III. Upstream-centered finite-difference schemes for ideal compressible flow. *Journal of Computation Physics*, vol. 23, p263-75, 1977.
15. Roe, P.L., Characteristic-based schemes for the Euler equations, *Ann. Rev. Fluid Mech*., vol. 18, p337,1986.
16. Lien, F.S., and Leschziner, M.A., Upstream monotonic interpolation for scalar transport with application to complex turbulent flows, *Int. J. Num. Meth. Fluids*, **19**, p527,1994
17. Sandia National Laboratories, Engine Combustion Network (public.ca.sandia.gov/ecn), 2008.
18. Nordin, N., Complex Chemistry Modeling of Diesel Spray Combustion, PhD Thesis, Chalmers Tekniska Högskola, Göteborg, 2001.